Syst. Biol. 61(5):913–926, 2012

DOI:10.1093/sysbio/sys039
Advance Access publication on March 20, 2012

The Pipid Root

ADAM J. BEWICK[1], FRÉDÉRIC J. J. CHAIN[1,3], JOSEPH HELED[2], AND BEN J. EVANS[1,*]

[1]*Department of Biology, Life Sciences Building Room 328, McMaster University, 1280 Main Street West Hamilton, ON L8S 4K1, Canada;* [2]*Department of Computer Science, University of Auckland, Auckland 1142, New Zealand; and* [3]*Present address: Department of Evolutionary Ecology, Max Planck Institute for Evolutionary Biology, August-Thienemann-Str. 2, 24306 Plön, Germany*

**Correspondence to be sent to: Department of Biology, 1280 Main Street West, LSB room 328, McMaster University, Hamilton, ON L8S4K1, Canada; E-mail: evansb@mcmaster.ca.*

Received 17 October 2011; reviews returned 13 February 2012; accepted 15 March 2012
Associate Editor: Richard Glor

Abstract.—The estimation of phylogenetic relationships is an essential component of understanding evolution. Accurate phylogenetic estimation is difficult, however, when internodes are short and old, when genealogical discordance is common due to large ancestral effective population sizes or ancestral population structure, and when homoplasy is prevalent. Inference of divergence times is also hampered by unknown and uneven rates of evolution, the incomplete fossil record, uncertainty in relationships between fossil and extant lineages, and uncertainty in the age of fossils. Ideally, these challenges can be overcome by developing large "phylogenomic" data sets and by analyzing them with methods that accommodate features of the evolutionary process, such as genealogical discordance, recurrent substitution, recombination, ancestral population structure, gene flow after speciation among sampled and unsampled taxa, and variation in evolutionary rates. In some phylogenetic problems, it is possible to use information that is independent of fossils, such as the geological record, to identify putative triggers for diversification whose associated estimated divergence times can then be compared a posteriori with estimated relationships and ages of fossils. The history of diversification of pipid frog genera *Pipa*, *Hymenochirus*, *Silurana*, and *Xenopus*, for instance, is characterized by many of these evolutionary and analytical challenges. These frogs diversified dozens of millions of years ago, they have a relatively rich fossil record, their distributions span continental plates with a well characterized geological record of ancient connectivity, and there is considerable disagreement across studies in estimated evolutionary relationships. We used high throughput sequencing and public databases to generate a large phylogenomic data set with which we estimated evolutionary relationships using multilocus coalescence methods. We collected sequence data from *Pipa*, *Hymenochirus*, *Silurana*, and *Xenopus* and the outgroup taxon *Rhinophrynus dorsalis* from coding sequence of 113 autosomal regions, averaging ∼300 bp in length (range: 102–1695 bp) and also a portion of the mitochondrial genome. Analysis of these data using multiple approaches recovers strong support for the ((*Xenopus*, *Silurana*)(*Pipa*, *Hymenochirus*)) topology, and geologically calibrated divergence time estimates that are consistent with estimated ages and phylogenetic affinities of many fossils. These results provide new insights into the biogeography and chronology of pipid diversification during the breakup of Gondwanaland and illustrate how phylogenomic data may be necessary to tackle tough problems in molecular systematics. [Coalescence; gene tree; high-throughout sequencing; lineage sorting; pipid; species tree; *Xenopus*.]

Estimation of phylogenetic relationships among species using molecular data must overcome challenges associated with estimating individual genealogies (e.g., phylogenetic error stemming from short branch lengths or homoplasy) and challenges associated with discordance between gene trees and species trees. Differences between gene trees and species trees can have a biological basis, including ancestral polymorphism, simultaneous divergence of multiple species (hard polytomies), and other phenomena such as balancing selection, gene conversion, horizontal gene transfer, interspecies hybridization, and allopolyploidization (Ioerger et al. 1990; Maddison 1997; Brooks and McLennan 2002; Evans 2008; Degnan and Rosenberg 2009). When ancestral population size is large, structured, or when the time between internodes is brief, genealogical discordance with a species tree can be common. Gene trees and species trees are similar when internal branch lengths are on the order of $\sim 5 \times 2N_e$ generations (Degnan and Salter 2005) but tend to differ when internal branch lengths are brief and when population size is large. Strikingly, for some asymmetrical species trees with short internodes, the most likely gene tree may not be the same as the species tree (Degnan and Rosenberg 2006) because the probability of a symmetrical (balanced) tree is greater than an asymmetrical (unbalanced) one (Rosenberg 2002). When the most likely gene tree is different from the species tree, the gene tree is said to be "anomalous" (Degnan and Rosenberg 2006). Mutational variance increases the parameter space that anomalous gene trees are observed, although this effect is offset by many anomalous trees being unresolved because of short internal branch lengths (Huang and Knowles 2009). Disparities between gene trees and species trees can also have an analytical basis, including phylogenetic error (Hillis et al. 1994) and inappropriate homology statements due to gene duplication or incorrect sequence alignment (Wong et al. 2008). Together, these factors can lead to incorrect inferences of topology, branch lengths, credible intervals, and parameter values of species trees.

Another challenge to understanding evolutionary history is the estimation of divergence times. Molecular clocks that use fossils for calibration generally rely on (i) an inference of phylogenetic affinities between a fossil and the group of extant species and (ii) an inference of the age of the fossil. Even if phylogenetic affinities and ages of fossils are well characterized, in most situations a fossil provides only a minimum (most recent) divergence time for a particular node. Geological calibrations

suffer from similar challenges and often provide minimum divergence times based on an assumption that diversification was either triggered by or preceded some event, such as the drifting apart of continental plates. Geological calibrations can potentially provide a maximum (most ancient) limit to the timing of divergence. For example, ignoring ancestral polymorphism, divergence of a terrestrial island endemic from a sister lineage on a continent could be assumed to have occurred more recently than the age of the island. Ancient DNA provides a third tool for calibration of molecular clocks. This information is perhaps optimal if its source is a direct ancestor of an extant species—a condition rarely met by most studies. In general, resources available for calibration of many groups are sparse, and the resulting calibrations can be vague or misleading.

An interesting example of these challenges is presented by the diversification of genera of the frog family Pipidae. Phylogenetic relationships among these taxa are unresolved and their resolution faces many of these topological and temporal challenges despite a relatively rich fossil record and a putative role for well-timed geological events in their diversification. There are 5 pipid genera: *Xenopus*, *Silurana*, *Hymenochirus*, *Pseudhymenochirus*, and *Pipa*, which include 19, 2, 4, 1, and 7 described species, respectively (Frost 2011). *Pipa* occurs in South America and the others are found in sub-Saharan Africa. Pipids are suspected to have drifted apart ∼100 Ma (Fig. 2; Cannatella and de Sá 1993; Roelants et al. 2007). Various studies have supported the (*Pipa* (*Hymenochirus* (*Xenopus, Silurana*))) topology (Roelants and Bossuyt 2005; Roelants et al. 2007; Irisarri et al. 2011; Pyron and Wiens 2011; Wiens 2011), the (*Hymenochirus* (*Pipa* (*Xenopus, Silurana*))) topology (Frost et al. 2006), and the ((*Hymenochirus*, *Pipa*)(*Xenopus, Silurana*)) topology (Báez and Pugener 2003; Evans et al. 2004, 2005; Trueb et al. 2005; Trueb and Báez 2006). These studies are not independent because many use data from the same genes, notably mitochondrial DNA and the autosomal locus RAG1. Nonetheless, these contradictions raise the possibility that internodes at the base of the pipid phylogeny are short, that the ancestral population sizes of pipid lineages were large or some combination.

Although some nodes are unresolved, a consensus has been reached about other aspects of pipid phylogeny (reviewed in Evans 2008). It is widely accepted that each genus is monophyletic, that (*Xenopus* + *Silurana*) is a clade, that (*Hymenochirus* + *Pseudhymenochirus*) is a clade, and most studies agree that Pipidae is the sister clade to the New World frog family Rhinophrynidae (Kluge and Farris 1969; Lynch 1973; Trueb and Cannatella 1986; Cannatella and Trueb 1988a, 1988b; Cannatella and de Sá 1993; Ford and Cannatella 1993; Graf 1996; Kobel et al. 1998; Evans et al. 2004; Roelants and Bossuyt 2005; Frost et al. 2006; Roelants et al. 2007; Irisarri et al. 2011; Pyron and Wiens 2011; Wiens 2011). An analysis of morphological characters by Cannatella and Trueb (1988a, 1988b) suggested that *Xenopus* is sister to a clade containing (*Silurana* + *Hymenochirus* + *Pipa*) but a reevaluation of these characters and molecular data by Cannatella and de Sá (1993) found (*Xenopus* + *Silurana*) to be monophyletic with respect to *Hymenochirus*. A phylogeny illustrating resolved and unresolved relationships among pipid frogs is presented in Figure 1, along with names for resolved nodes following Cannatella and de Sá (1993). As pointed out by Frost et al. (2006), resolution of phylogenetic relationships among pipids may boil down to ascertaining where the root is in only 1 of the 3 possible unrooted topologies for *Xenopus*, *Silurana*, *Hymenochirus*, and *Pipa* (topology 1 in Fig. 1).

With an aim of further exploring the controversial phylogenetic relationship of pipid frogs, we assembled a large multilocus data set using a combination of 454 pyrosequencing of cDNA and publicly available sequence data. We analyzed each locus individually and also jointly using coalescent-based approaches that accommodate differences between gene trees and species trees. We used a multilocus coalescent-based method (*BEAST) to develop a temporal framework for diversification based on the hypothesis that continental drift triggered cladogenesis of one or more lineages in this group. We then used the relatively rich fossil record of these frogs to evaluate a posteriori the plausibility of these proposed geological mechanisms for diversification. We uncovered a high degree of genealogical discordance among loci, underscoring the utility of phylogenomics and non-concatenated analyses for contextualizing the evolutionary history of this group.

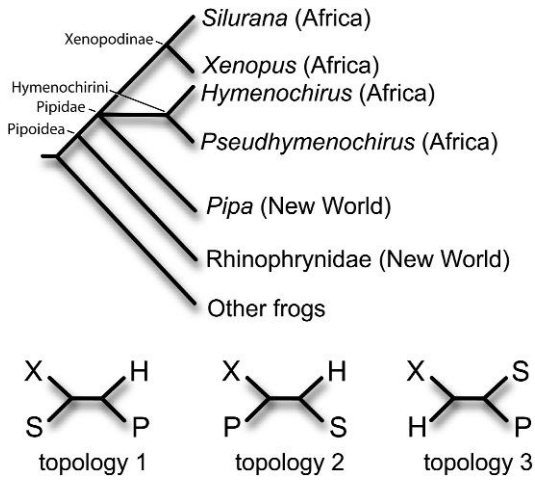

FIGURE 1. Monophyly of *Silurana* + *Xenopus*, of *Hymenochirus* + *Pseudhymenochirus*, and of Pipidae + Rhinophrynidae has been established based on morphological and molecular data, but relationships among 3 major lineages within the frog family Pipidae remain unresolved. Node-based names of clades are indicated on the topology. Topologies 1–3 are the 3 possible unrooted topologies for *Silurana* (S), *Xenopus* (X), *Pipa* (P), and *Hymenochirus* (H); the available data supports unrooted topology 1. The genus *Pseudhymenochirus* and the family Rhinophrynidae both include only one species (*Pseudhymenochirus merlini* and *Rhinophrynus dorsalis*, respectively).

Materials and Methods

Taxon Sampling and Multilocus Data

We collected multilocus sequence data from the pipid frogs *Xenopus laevis*, *Silurana tropicalis*, *Hymenochirus curtipes*, *Pipa carvalhoi*, and the outgroup taxon *Rhinophrynus dorsalis*. Data from *X. laevis* and *S. tropicalis* were obtained from GenBank; most data from the other species were obtained by 454 pyrosequencing of cDNA. An *H. curtipes* individual and a *P. carvalhoi* individual of unknown geographic origin were obtained from animal suppliers (PetSmart and Xenopus Express, respectively), and a sample of *R. dorsalis* was obtained from the tissue archive at the Museum of Vertebrate Zoology at the University of California at Berkeley. We also included data from 6 autosomal loci and one mitochondrial region that were available in GenBank.

For 454 pyrosequencing, total RNA was extracted using QIAGEN RNeasy Mini Kit from liver tissue. Normalized double-stranded cDNA was prepared using SMART cDNA Synthesis Kit (Clontech) and Advantage 2 PCR Kit, and TRIMMER cDNA Normalization Kit (Evrogen), according to the manufacturer's protocol and as described in Chain et al. (2008). The normalized cDNA was used for 454 pyrosequencing (ROCHE GS FLX). A titration run was performed for four 1/16th portions of a plate for each of 3 species (*H. curtipes*, *P. carvalhoi*, and *R. dorsalis*) and an additional 1/4th portion of a plate with the appropriate titration was then run for each species.

Contigs were assembled from the 454 data using GS De novo Assembler (Roche). We averaged 5, 20, and 29 reads per locus for *R. dorsalis*, *P. carvalhoi*, and *H. curtipes*, respectively, and single reads were used for portions of some loci for some species (Supplementary Table 1, Dryad database: doi: 10.5061/dryad.bt92r9f1). The lower coverage of *R. dorsalis* is probably related to the lower quality of cDNA synthesized from this old flash frozen sample. Single nucleotide polymorphisms in the resulting contigs were encoded using International Union of Pure and Applied Chemistry (IUPAC) nucleotide codes. Custom Perl scripts and MUSCLE version 3.6 (Edgar 2004) were used to align the data to *X. laevis* and *S. tropicalis* sequences from GenBank, retaining as putative orthologs those sequences that all had the reciprocal best BLAST hit (Altschul et al. 1997). Our previous studies used this approach to identify putative singletons and duplicates in *X. laevis* (Chain and Evans 2006; Chain et al. 2008, 2011), and the resulting data sets are highly concordant with other independent studies (Morin et al. 2006; Hellsten et al. 2007; Sémon and Wolfe 2008) and with NCBI's UniGene database. For *X. laevis*, a tetraploid species, we identified 2 paralogs for most loci. In order to have the same number of terminals for all loci in our analysis, we randomly selected one *X. laevis* paralog to be included. Both *X. laevis* paralogs are monophyletic with respect to other pipid genera because they formed by genome duplication in *Xenopus* that occurred after divergence from *Silurana* (Evans et al. 2005; Evans 2007; Bewick et al. 2011). Thus, discarding one paralog from *X. laevis* should have no impact on our inferences of evolutionary relationships among pipid genera.

When analyzing sequences from species as diverged as those in this study, homology statements (alignment) of sequence data can be challenging. For this reason, all noncoding sequences from the 5′ or 3′ untranslated region were discarded and alignments were adjusted manually with MacClade version 4.08 (Maddison and Maddison 2000) using codon frame inferred from complete transcripts of *Xenopus* and *Silurana* to facilitate homology statements. We retained only alignments with complete information from all 5 focal taxa and a length of at least 99 bp that was devoid of stop codons in all taxa. The only gaps in the alignments in the nuclear data are due to amino acid insertion/deletion polymorphisms, which were infrequently encountered.

One concern is that some of the data partitions could inadvertently include paralogous instead of orthologous sequences. Because we have large databases from *X. laevis* and *S. tropicalis*, we can be fairly confident that the reciprocal best BLAST hits between these species are orthologous. However, as illustrated in Figure 3a–c, it is conceivable that we included nonorthologous sequences from *Pipa*, *Hymenochirus*, or *Rhinophrynus* due to gene duplication or missing data. Even without missing data, it is also conceivable that incomplete lineage sorting could cause a *R. dorsalis* sequence to be an inappropriate outgroup, even though this species is sister to pipids (Fig. 3d). One possible signal of non-orthology or incomplete lineage sorting in the outgroup would be an atypically low or high divergence between one or more ingroup sequence(s) and the outgroup sequence compared with the other ingroup sequences (Fig. 3). To identify alignments that potentially contain nonorthologous sequences, we therefore calculated a Jukes–Cantor corrected pairwise distance between each ingroup sequence and the outgroup sequence using PAUP* (Swofford 2002). We then divided each of these 4 distances by their maximum to generate a "standardized outgroup distance ratio" for each ingroup taxon. With equal rates of evolution among orthologous sequences, each standardized outgroup distance ratio should be near one, and departures from one would be due to stochastic variation in mutation. If nonorthologous sequences are present, one or more standardized outgroup distance ratios should be low. For example in Figure 3a, the standardized outgroup distance ratio between *Hymenochirus* and the outgroup would be lower than those between *Xenopus*, *Silurana*, or *Pipa* and the outgroup. Likewise in Figure 3b, the standardized outgroup distance ratio between *Hymenochirus* and the outgroup would be the highest (and therefore equal to one) and the others would be much lower than one. Thus, as a conservative measure, we removed from the analysis all loci with a standardized outgroup distance ratio less than 0.4. This cutoff was arbitrary and is independent of the phylogeny supported by each locus. By imposing this cutoff, we excluded

14 data partitions with high similarity between at least one ingroup sequence and the outgroup sequence compared with the other ingroup sequences. The autosomal portion of the data set thus comprised portions of 114 loci, which are treated as 113 loci because the tightly linked genes RAG1 and RAG2 were treated as a single locus.

We also included in our analysis portions of a ~2400 bp sequence from the 12S and 16S rDNA genes and the $tRNA^{val}$ of the mitochondrial genome (Evans et al. 2004). To facilitate unambiguous alignment, we discarded loop regions of these rDNA enzymes based on an analysis of secondary structure (Cannone et al. 2002). To avoid violation of the assumption of independent evolution of each site, we discarded half of the stem sequences that paired with the retained portion of the data set, leaving a total of 432 bp. These mitochondrial data are therefore composed exclusively of independently evolving stem region sites that do not form doublets with each other. Six sites in the mitochondrial DNA alignment had gaps as a result of length variation at the junction with a loop region.

Gene Tree Estimation

We estimated phylogenies from each locus independently with Bayesian analysis as implemented by MrBayes version 3.1.2 (Huelsenbeck and Ronquist 2001) using a model of evolution selected by the Akaike Information Criterion (AIC) with MrModelTest version 2 (Nylander 2004). Similar to the BEST analyses described below, these models were not partitioned by codon position. Two Markov Chain Monte Carlo (MCMC) runs were performed with 4 chains per run, each for 10 million generations, with the temperature parameter set to 0.2. Based on inspection of the posterior likelihood surface with Tracer version 1.5 (Drummond and Rambaut 2007), a burn-in of 2 million generations was discarded for all individual locus analyses. The effective sample size (ESS) of the post burn-in parameter MCMC sampling was calculated using Tracer and an ESS value >200 was used as an indication that the MCMC sample had converged on the posterior distribution. These and other computationally intensive analyses were performed on the sharcnet computer cluster (www.sharcnet.ca) and also the computer network of Brian Golding at McMaster University.

Concatenated Analysis

Under situations where discordance between gene trees and a species tree is expected, concatenation of sequence data with different evolutionary histories can distort branch lengths, relationships, and credibility intervals recovered from phylogenetic analysis (Kubatko and Degnan 2007). Nonetheless, for comparative purposes, we performed a partitioned analysis on the concatenated data using the preferred model of evolution for each locus as ascertained with the AIC. Two MCMC runs, each with 4 chains for 20 million generations, were performed. A burn-in of 2 million generations was discarded and convergence assessed based on the Tracer analysis discussed above.

*Species Tree Estimation—BEST and *BEAST*

We used Bayesian estimation of species trees (BEST) version 2.3 (Liu and Pearl 2007) and *BEAST pre-release version 1.7.0 (Drummond and Rambaut 2007; Heled and Drummond 2010) to estimate a species tree from the multilocus data. These methods assume that discrepancies between gene trees and the species tree are due exclusively to lineage sorting, free recombination between genes, no recombination within genes, and no gene flow after speciation. In both of these analyses, the tree topologies are unlinked across partitions (i.e., estimated independently for each gene) and a species tree is estimated from these potentially discordant tree topologies.

For both analyses, we evaluated 3 models of evolution using Bayes factors as described by Nylander et al. (2004). For the BEST analysis, the first model (hereafter JC $+\Gamma+$ f) employed an equal transition rate among nucleotides, with a Γ—distributed rate heterogeneity and base frequencies estimated from the data with a Dirichlet prior. The second model (hereafter HKY $+\Gamma+$ f) was the same as the first except that the substitution rates between transitions and transversions were estimated separately. The third model (hereafter GTR $+\Gamma+$ f) is the same as the first except that the transition rates between each nucleotide were estimated separately. For all analyses, the parameter estimations were performed independently for each partition and the gene mutation prior was set at (0, 114) to conservatively allow for a different mutation rate for each partition. The prior for the effective population size parameter theta (Θ) was inverse gamma (3, 0.018) based on silent site nucleotide diversity in *X. laevis* (Bewick et al. 2011) as suggested in the program documentation. Depending on the model, multiple independent MCMC runs were performed (37 for JC $+\Gamma+$ f, 33 for HKY $+\Gamma+$ f, and 41 for GTR $+\Gamma+$ f), each with 2 chains that were initiated at different starting seeds for at least 40 million generations, sampling every 2000 generations, with the temperature parameter set to 0.20, *R. dorsalis* set as the outgroup, the mtDNA partition set as haploid, and the other partitions set as diploid. To assess convergence of the MCMC runs, we first inspected a plot of the posterior distribution of likelihoods from each independent MCMC chain and based on this inspection, we discarded 4–70 million generations as burn-in. We then calculated the ESS of the post burn-in parameter values from all runs using Tracer and convergence of the MCMC run on the posterior distribution was again assumed when ESS values exceeded 200.

We also used *BEAST pre-release version 1.7.0 (Drummond and Rambaut 2007; Heled and Drummond 2010)

to estimate a species phylogeny and provide estimates of divergence times based on geological calibration points enumerated below. We again set out to consider 3 models of evolution using the approach of Nylander et al. (2004) but for this analysis the models were more complex. All the *BEAST models estimated parameters for each codon position of each partition separately. They differed in whether a single rate was used for nucleotide transitions (hereafter JC codon), 2 separate rates for transitions and transversions (hereafter HKY codon), or separate rates for all transitions and transversions (hereafter GTR codon). Because the mtDNA data were from stem regions only, we did not use a codon model on this partition. For all models, base frequencies were assumed to follow the empirical proportions. A correction term was applied to the default pure birth (Yule) prior, ensuring that the marginal density of the combined prior was identical to the calibration density (Heled and Drummond 2011). This is in contrast to the default BEAST construction which results in a prior that neither preserves the calibration densities nor the Yule prior (Heled and Drummond 2011). The correction terms are described in further detail in Supplementary information for each of the 3 calibration regimes discussed below. The prior on birth rate x was set to the uninformative $1/x$ with a hard bound of (0.0007,1) and the prior on the evolutionary rate y was set to the uninformative $1/y$. Each partition had one rate parameter and 3 "subrates" for each codon position, with either the Jukes–Cantor, HKY, or GTR model for each codon position. *Rhinophrynus dorsalis* was set as the outgroup by enforcing monophyly of Pipidae. Ploidy of mitochondrial DNA was set to haploid and all other loci to diploid and a strict molecular clock was assumed. For each *BEAST analysis, dozens of independent runs were performed, each for at least 200 million generations. A burn-in of 5–80 million generations was discarded based on inspection of the posterior likelihoods using Tracer. Convergence was evaluated using ESS values after discarding burn-in generations that were identified by eye as described above.

We considered 2 geological calibration points in the *BEAST analysis (Fig. 2). The first hypothesizes that divergence of *Pipa* from other pipids was triggered by the rifting apart of South America and Africa. From the Late Jurassic through the Middle Cretaceous, South America and Africa were a continuous landmass called West Gondwana (Smith et al. 1994; Gheerbrant and Rage 2006). Based on dates provided by previous studies (Pitman et al. 1993; Maisey 2000; McLoughlin 2001; Sereno et al. 2004; Ali and Aitchison 2008), we assigned a normal prior for this divergence time with a mean of 102 Ma and a standard deviation of 7 myr in order to accommodate uncertainty in this estimate. The second calibration point hypothesizes that pipoid divergence into the families Rhinophrynidae and Pipidae was triggered by the opening of the North Atlantic Ocean as North America rifted apart from West Africa (Duellman and Trueb 1994). This occurred during the Late Jurassic (McHone and Butler 1984) and we again

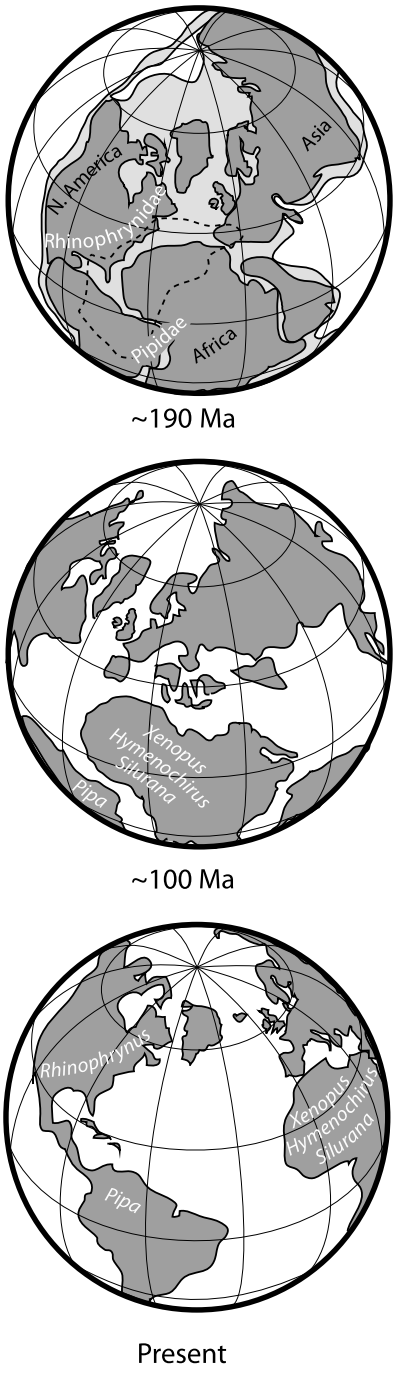

FIGURE 2. Evolution of the Atlantic ocean and of pipoid frogs: our geological calibration points hypothesize that cladogenesis of pipoids was influenced by continental drift. Roughly 190 Ma, divergence of Rhinophrynidae and Pipidae may have been triggered by the opening of the North Atlantic Ocean and consequent separation of North America and West Africa. The Central Atlantic Magnetic Province associated with this event is depicted with dotted lines and putative land positive regions in light gray following Korte et al. (2009) and McHone (2000). About 100 Ma, divergence of *Pipa* from African pipids may have been triggered by the rifting apart of South America and Africa. Pipoid genera now occur in North America, South America, and Africa.

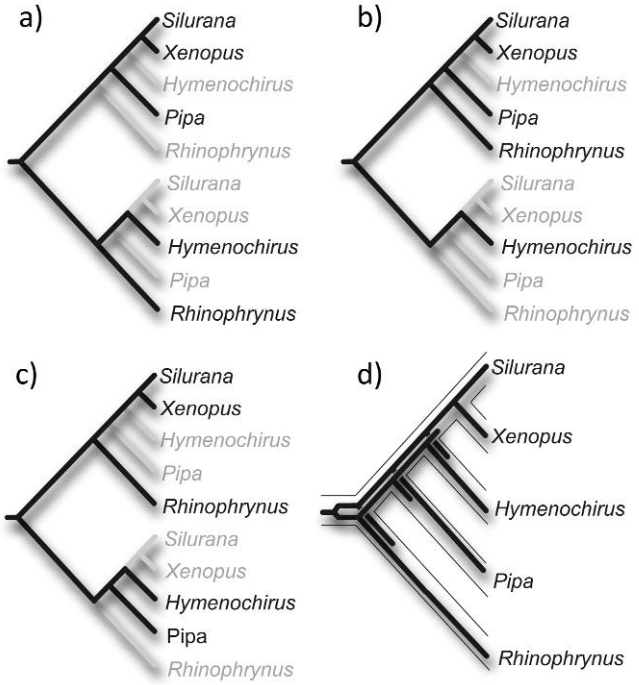

FIGURE 3. Gene family extinction or missing data could generate misleading phylogenetic affinities. In (a–d), the example "true" phylogeny is (*Pipa* (*Hymenochirus* (*Xenopus*, *Silurana*))). However, as a consequence of unsampled orthologs in (a) and (b), rooting the phylogeny with the *Rhinophrynus* sequence suggests that *Pipa* is sister to (*Xenopus* + *Silurana*). In (c), rooting the phylogeny with the *Rhinophrynus* sequence suggests that (*Hymenochirus* + *Pipa*) and (*Xenopus* + *Silurana*) are reciprocally monophyletic. In (d), ancestral polymorphism causes the topology rooted with *Rhinophrynus* sequences to be (*Hymenochirus* (*Pipa* (*Xenopus*, *Silurana*))). In (a–d), divergence between *Rhinophrynus* and some ingroup taxa is lower than that between *Rhinophrynus* and other ingroup taxa, an observation we exploit with the standardized outgroup distance ratio.

used a normal prior for this divergence time with a mean of 190 Ma and the same standard deviation (7 myr) in order to accommodate uncertainty (Withjack et al. 1998). We performed 3 *BEAST analyses—one with each of these calibration points (*BEAST analysis 1 and 2, respectively) and one with both (*BEAST analysis 3).

RESULTS

Using data from GenBank and 454 pyrosequencing, we generated 114 5-taxon alignments for *X. laevis*, *S. tropicalis*, *H. curtipes*, *P. carvalhoi*, and the outgroup taxon *R. dorsalis* for a combined total of 35,673 bp per taxon. This included sequences from the coding region of 114 nuclear loci (2 of which were linked and thus concatenated) and a portion of rDNA sequence from the mitochondrial genome in which sites evolve independently. Each data partition has sequence from all 5 taxa and there, therefore, are no missing data in this study. A total of 9106 positions (25.5%) were variable including 5940 (16.6%) that were parsimony uninformative and 3166 (8.9%) that were parsimony informative. Fifty-eight nucleotides in the data set were encoded with ambiguous IUPAC symbols. A summary of variation in partition sequence length is presented in Figure 4a and additional information on each partition and GenBank accession numbers for sequences >200 bp in length are available in Supplementary information. Input files for BEST and *BEAST that include all sequences are available in the Dryad database: doi: 10.5061/dryad.bt92r9f1.

Figure 4b illustrates how the minimum standardized outgroup distance ratio varied among the different data partitions with respect to the length of each partition. Shorter alignments tended to have higher variance in standardized outgroup distance ratios. Higher variance is expected for shorter alignments, but this could also suggest that non-orthologous sequences are more prevalent in the shorter alignments.

Analysis of Individual and Concatenated Loci

The posterior distribution of a phylogenetic tree can be summarized either with the posterior distribution of tree topologies or with the posterior distribution of clades (Sukumaran and Linkem 2009). The former is accomplished by counting how many times each possible topology appears in the posterior distribution with the most common topology being the maximum a posterior probability tree (hereafter the MAP tree). The latter is accomplished by counting how many times each possible clade appears in the posterior distribution and is commonly summarized with a majority rule consensus topology. Most studies focus on the posterior distribution of clades, in part because many distinct tree topologies are present in posterior distributions of analyses with many taxa. For this reason, the majority rule consensus topology may differ from the MAP tree. Here, we discuss both types of summaries because the posterior distribution includes only 15 possible topologies due to the small number of ingroup taxa.

Figure 5 summarizes the posterior distribution of tree topologies recovered from individual Bayesian analysis of each of the 114 data partitions. Analysis of individual loci illustrates that 3 of the 5 possible rootings of topology 1 in Figure 1 are far more probable than the other 2 possible rootings of topology 1 or than any of the rootings of topologies 2 and 3. Of the 5 possible rootings of topology 1 in Figure 1, only 3—((*Xenopus*, *Silurana*)(*Pipa*, *Hymenochirus*)), (*Pipa* (*Hymenochirus* (*Xenopus*, *Silurana*))), and (*Hymenochirus* (*Pipa* (*Xenopus*, *Silurana*)))—account for 80.5% of the combined post-burn-in posterior probability distribution of topologies across all individual loci. The breakdown of this distribution is 28.8% for the ((*Xenopus*, *Silurana*)(*Pipa*, *Hymenochirus*)) topology, 26.7% for the (*Pipa* (*Hymenochirus* (*Xenopus*, *Silurana*))) topology, and 25.0% for the (*Hymenochirus* (*Pipa* (*Xenopus*, *Silurana*))) topology. The remaining 19.5% consisted of the other 12 possible rooted topologies.

The MAP tree was ((*Xenopus*, *Silurana*)(*Pipa*, *Hymenochirus*)) for 39 loci, (*Pipa* (*Hymenochirus* (*Xenopus*, *Silurana*))) for 28 loci, and (*Hymenochirus* (*Pipa* (*Xenopus*, *Silurana*))) for 27 loci. However, the ((*Xenopus*,

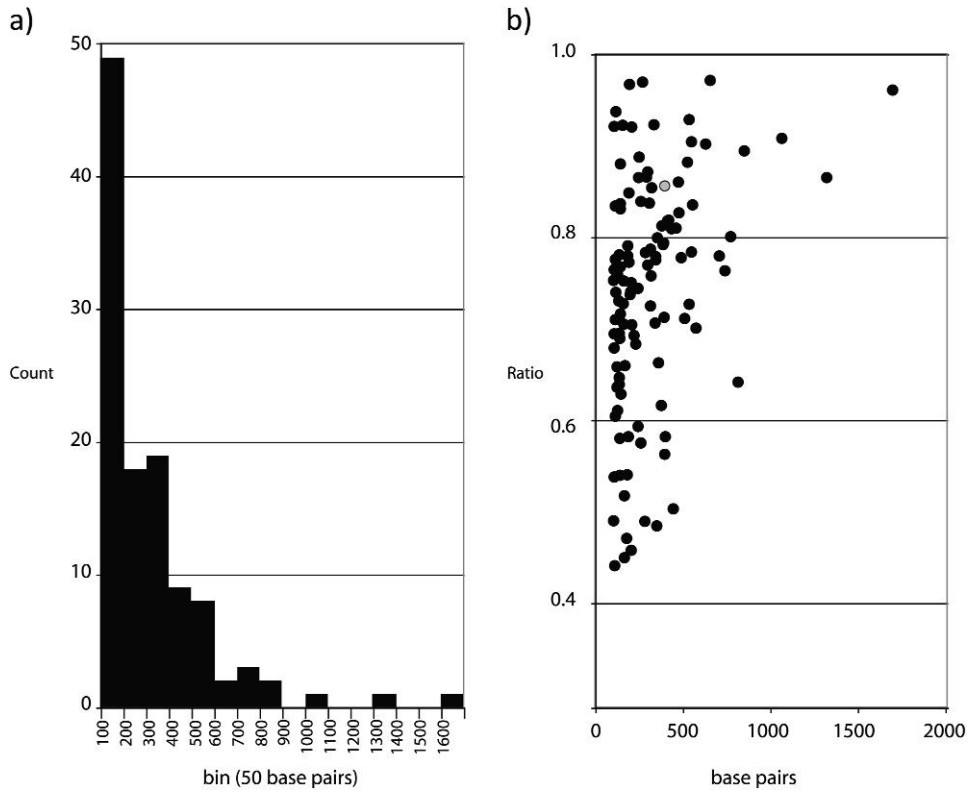

FIGURE 4. Descriptive information about data analyzed in this study. (a) Distribution of the sizes of the data partitions. (b) The standardized outgroup distance ratio, that is the ratio of the lowest Jukes–Cantor-corrected pairwise distances between each ingroup taxon and the outgroup divided by the highest pairwise distance, as a function of the size in base pairs of each partition. In (b), mitochondrial DNA is indicated with a gray circle.

Silurana)(*Pipa*, *Hymenochirus*)) topology comprises >80% of the posterior topology distribution for 13 partitions, but the (*Pipa* (*Hymenochirus* (*Xenopus*, *Silurana*))) and (*Hymenochirus* (*Pipa* (*Xenopus*, *Silurana*))) do not comprise >80% of the posterior topology distribution for any partition (Fig. 5). For the mitochondrial DNA partition, the ((*Xenopus*, *Silurana*)(*Pipa*, *Hymenochirus*)) comprised 83.7% of the posterior topology distribution, which is consistent with phylogenetic analysis of a larger portion of mitochondrial DNA sequence that includes rDNA stem and loop regions (Evans et al. 2004). Overall then, analysis of individual partitions suggests that the ((*Xenopus*, *Silurana*)(*Pipa*, *Hymenochirus*)) topology has the highest posterior probability.

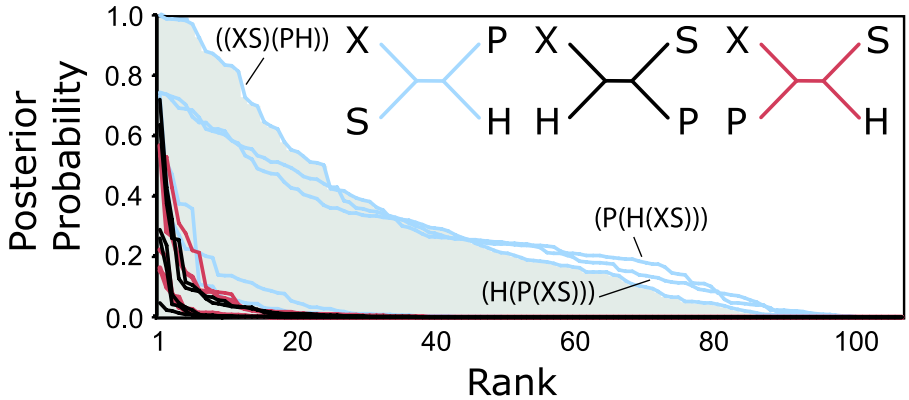

FIGURE 5. Posterior probability distribution of each of the 15 possible rooted topologies recovered from analysis of 114 individual alignments. For each rooted topology, the posterior probabilities (expressed as a decimal) from each partition were ranked from highest to lowest. Each set of 5 distributions are shaded according to their corresponding unrooted 4-taxon topology. The distribution for ((*Xenopus*, *Silurana*)(*Pipa*, *Hymenochirus*)) is shaded to emphasize that this topology is the only one that has strong support (posterior probability > 80) at multiple partitions. The next most strongly supported topologies are (*Pipa* (*Hymenochirus* (*Xenopus*, *Silurana*))) and (*Hymenochirus* (*Pipa* (*Xenopus*, *Silurana*))). Letters refer to taxa as defined in Figure 1.

We contrasted the MAP tree with the majority rule consensus topology for each partition. The ((*Xenopus*, *Silurana*)(*Pipa*, *Hymenochirus*)) consensus topology was recovered for 29 loci (including mtDNA), the (*Pipa* (*Hymenochirus* (*Xenopus*, *Silurana*))) consensus topology was recovered for 29 loci, and the (*Hymenochirus* (*Pipa* (*Xenopus*, *Silurana*))) consensus topology was recovered for 22 loci. The consensus topologies of 34 loci were either unresolved with respect to the trichotomy depicted in Figure 1 or were one of the other 12 possible topologies. The difference in support for the top 3 rooted topologies was not due to differences in the length of the alignments. The mean length of the loci with the ((*Xenopus*, *Silurana*)(*Pipa*, *Hymenochirus*)) consensus topology was 337 bp, whereas the mean length of the loci with the (*Pipa* (*Hymenochirus* (*Xenopus*, *Silurana*))) or (*Hymenochirus* (*Pipa* (*Xenopus*, *Silurana*))) consensus topologies was 381 and 334 bp, respectively. However, support for the other possible rooted topologies was probably related to differences in information content—the mean length of 34 loci with either an unresolved consensus tree or a consensus topology that was not ((*Xenopus*, *Silurana*)(*Pipa*, *Hymenochirus*)), (*Pipa* (*Hymenochirus* (*Xenopus*, *Silurana*))), or (*Hymenochirus* (*Pipa* (*Xenopus*, *Silurana*))) was only 221 bp. A concatenated MrBayes analysis of all partitions also produced a consensus topology with 100% posterior probability for the ((*Xenopus*, *Silurana*)(*Pipa*, *Hymenochirus*)) topology.

Multilocus Coalescent Analysis

Using Bayes factors, the GTR + Γ+ f was strongly favored for BEST analysis (Table 1) based on the criterion of Kass and Raftery (1995). Using this model, BEST analysis of the full data set recovered the ((*Xenopus*, *Silurana*)(*Pipa*, *Hymenochirus*)) consensus topology with 100% posterior probability for the (*Xenopus*, *Silurana*) clade and 95% posterior probability for the (*Pipa*, *Hymenochirus*) clade.

Our *BEAST analyses using the GTR codon model failed to converge for multiple parameters, even after sampling a large number of states in multiple independent runs. Thus, we focus our discussion on the next most complex model (HKY codon) in which analysis the MCMC chain converged on the posterior distribution for all parameters for each of the 3 differently calibrated analyses (Table 1). This model was preferred over the JC codon model according to the criterion of Kass and Raftery (1995) (Table 1). The topology of the species tree recovered from the HKY codon model in *BEAST was identical to that recovered from the GTR codon model in *BEAST even though most parameters did not converge in the GTR codon analysis. Results using the HKY codon model in *BEAST were also consistent with BEST analyses. Specifically, the ((*Xenopus*, *Silurana*)(*Pipa*, *Hymenochirus*)) topology was the most probable one and monophyly of *Xenopus* and *Silurana* was supported by 100% posterior probability in each of the 3 differently calibrated *BEAST analyses (Fig. 6). When only one calibration point was used (*BEAST analysis 1 or 2), posterior probability on the clade containing *Pipa* and *Hymenochirus* was 71% or 73%. When both calibration points were used the ((*Xenopus*, *Silurana*)(*Pipa*, *Hymenochirus*)) topology was even more strongly supported with 86% posterior probability on the clade containing *Pipa* and *Hymenochirus* (Fig. 6). In *BEAST analysis 1, divergence of *Xenopus* and *Silurana* was estimated to have occurred 50.4 Ma with a 95% credible interval of 38.6—63.2 myr. In *BEAST analyses 2 and 3, divergence estimates of *Xenopus* and *Silurana* were almost identical (∼65 Ma with a 95% credible interval of ∼57—74 Ma). In *BEAST analysis 1, estimated divergence time of the clade containing *Xenopus* and *Silurana*, hereafter "Xenopodinae" (Cannatella and de Sá 1993) from the clade containing *Pipa* and *Hymenochirus*, hereafter "Pipinae" (Cannatella and de Sá 1993), is 109.4 Ma with a 95% credible interval of 89.2–131.1 Ma. In *BEAST analyses 2 and 3, estimated divergence time of Xenopodinae from Pipinae are

TABLE 1. Statistics on coalescent-based analyses of species trees (BEST and *BEAST Analyses 1–3) including the model, the post burn-in log likelihood (-LnL), the number of states sampled (# States), 2 × log(Bayes Factor), the sample frequency (Sampling), the ESS of the likelihood (LnL ESS), and the number of parameters that had ESSs greater than 200 (ESS > 200), between 100 and 200 (100 < ESS < 200), and less than 100 (ESS < 100)

BEST model	-LnL	# States	2log(Bayes Factor)	Sampling	LnL ESS	ESS > 200	100 < ESS < 200	ESS < 100
JC + G + d	107,838	527,788,000	—	2000	400	56	134	45
HKY + G + d	105,564	885,066,000	4548	2000	961	147	89	0
GTR + G + d	105,203	1,336,892,000	722	2000	1389	241	0	0
*BEAST Analysis 1								
JC codon	101,887	1,935,300,000	—	25,000	23,962	931	0	0
HKY codon	97,481	2,009,100,000	8812	25,000	17,590	1271	0	0
*BEAST Analysis 2								
JC codon	101,165	1,929,025,000	—	25,000	25,116	931	0	0
HKY codon	97,482	2,147,475,000	7366	25,000	22,873	1271	0	0
*BEAST Analysis 3								
JC codon	101,867	1,987,000,000	—	25,000	24,326	931	0	2
HKY codon	97,481	2,147,475,000	8812	25,000	21,137	1271	0	0

Note: Values are not reported for the GTR codon model in *BEAST Analyses 1–3 because convergence was not achieved at most of the 2631 parameters.

similar (143.4 and 134.7 Ma with 95% credible intervals of 122.8–163.4 and 111.9–156.1 myr, respectively). In *BEAST analysis 1, estimated divergence time of Pipidae and Rhinophrynidae is 144.7 Ma with a 95% credible interval of 115.7–176.4 Ma.

The geological calibration points provide estimates of evolutionary rates that appear reasonable (Supplementary Fig. 1). Rates of evolution varies across partitions but are $\sim 4.7 \times 10^{-10}$ substitutions per site per year, assuming a generation time of 1 year. Interestingly, the rate of evolution of the stem region of mitochondrial DNA ribosomal genes appears to be similar to the rates of evolution of autosomal coding regions, even though the overall rate of mitochondrial DNA is faster than autosomal DNA in some groups, such as primates (Brown et al. 1982). Although we do not attempt to directly compare the models used by BEST and *BEAST, use of the codon model in the *BEAST analysis is probably preferable given the substantially different rates of evolution of each codon position (Supplementary Fig. 2). Taken together, analysis of the individual loci and the collective coalescent-based analyses provide strong support for the ((*Xenopus*, *Silurana*)(*Pipa*, *Hymenochirus*)) relationship. We relate divergence time estimates from the *BEAST analyses to geological and fossil information below.

Discussion

The complexity of the phylogenetic problem explored here is relatively simple in the sense that we seek to estimate relationships among only 4 lineages (4 genera of frogs in the family Pipidae) and there are therefore only 3 possible unrooted topologies (Fig. 1) and only 15 possible rooted topologies. However, these relationships are actually quite difficult to resolve because they are old, because the internodes are probably short, and because ancestral populations were probably very large and/or structured. Our analyses (Figs. 5 and 6) support the contention of Frost et al. (2006) that the primary challenge to resolving relationships among pipids is locating the position of the root of only one of the 3 possible unrooted topologies (topology 1 in Fig. 1). Using a combination of publicly available sequences, new data from 454 pyrosequencing, and multilocus coalescent phylogenetic analysis, the relationship ((*Xenopus*, *Silurana*)(*Pipa*, *Hymenochirus*)) is most strongly supported. Thus, the pipid root is on the lineage connecting Xenopodinae and Pipinae (Fig. 1). This result is consistent with the morphology-based results of Báez and Pugener (2003), Trueb et al. (2005), and Trueb and Báez (2006), a mitochondrial DNA analysis by Evans et al. (2004), an analysis of one autosomal gene by Evans et al. (2005), and a maximum parsimony analysis of concatenated autosomal loci by Roelants and Bossuyt (2005). However, it is not consistent with the results of Frost et al. (2006) or various maximum likelihood analyses (Roelants and Bossuyt 2005; Roelants et al. 2007; Irisarri et al. 2011; Pyron and Wiens 2011). What could account for these discrepancies?

For a 3-taxon problem, even when internodes are short, each possible gene topology is equally likely so anomalous gene trees do not exist (Degnan and Rosenberg 2006). If we accept the uncontroversial relationships depicted in Figure 1, the phylogenetic issue addressed in this study boils down to a 3-taxon problem with no anomalous trees. However, if we do not assume *Xenopus* + *Silurana* to be a clade for all portions of their genomes, this becomes a 4-taxon problem and an "anomaly zone" may exist depending on the length of the internodes (Degnan and Rosenberg 2006). However, analysis of individual loci suggests that anomalous gene trees had very little impact on our phylogenetic inference. If anomalous gene trees were common, one would expect similar frequencies of all possible rootings of each of the 3 unrooted topologies depicted in Figure 1, but this is not the case (Fig. 5). Instead, most (80.5%) of this distribution is comprised of only 3 alternative rootings of only one labeled unrooted topology (topology 1 in Fig. 1), with the other 12 rootings being very rare in the posterior distribution.

Here, it was not possible to estimate effective population size for the extant species because we lack intraspecific data, but we are able to get rough estimates of the ancestral population size of the ancestral nodes. In all *BEAST analyses, the estimated ancestral population size of Xenopodinae is the lowest (~10 million individuals) and that of pipoids (the most recent common ancestor of *Rhinophrynus*, *Pipa*, *Hymenochirus*, *Pseudhymenochirus*, *Xenopus*, and *Silurana*) is second lowest (~26 million individuals). When only one node is fixed for calibration, the effective population size of Pipinae is smaller (~75 million individuals) than that of Pipidae (the most recent common ancestor of *Xenopus*, *Silurana*, *Pipa*, *Hymenochirus*) (~81 million individuals) but when both calibration points are enforced the opposite is true (163 and 107 million individuals for Pipinae and Pipidae, respectively). The relative magnitudes of these estimates in comparison to the ancestor of Xenopodinae are consistent with the observation that most genealogical discordance involves the location of the pipid root (i.e., whether or not "Pipinae" is a clade). These estimated ancestral population sizes are huge and this is unexpected in frogs and even high for some species of fruit flies. This may be a result of the sensitivity of *BEAST to the absence of intraspecific polymorphism data, a lack of phylogenetic signal in some partitions (which increases genealogical discordance), nonneutral evolution of portions of the sequences, or nonorthology of some sequences. Another important factor is that these ancestral populations were probably not panmictic and that ancestral population structure has the potential to inflate inferred effective population sizes (Wright 1943; Nei and Takahata 1993). This last possibility seems particularly plausible given the enormous distribution of ancestral pipoids which spanned much of North America, Europe, the Middle East, Africa, and South America (Trueb et al. 2005). Using different methods, a recent analysis of ancestral effective population size of 2 subdivided species of

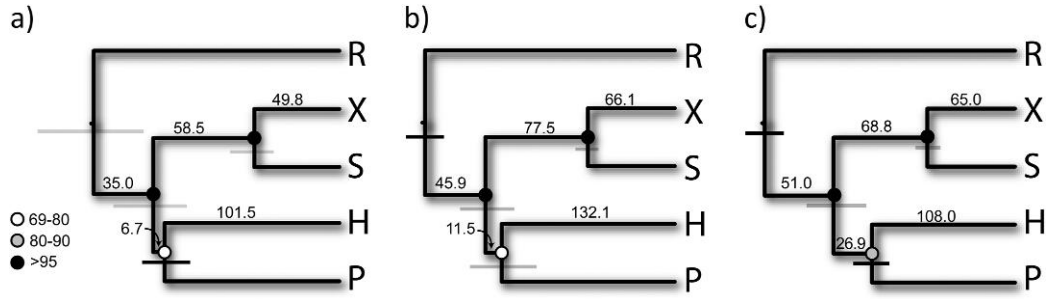

FIGURE 6. Consensus species trees from (a) *BEAST Analysis 1 which uses only the calibration for divergence of *Pipa* from *Hymenochirus*, (b) *BEAST Analysis 2 which uses only the calibration for divergence of Rhinophrynidae from Pipidae, and (c) *BEAST Analysis 3 which uses both of these calibrations. Numbers above branches represent time in millions of years and posterior probabilities (expressed as percentages) are indicated by shaded circles over each node. Gray bars represent the 95% highest posterior density intervals for time estimates in the posterior distribution and dark bars represent the nodes that were fixed in each analysis. Letters refer to taxa as defined in Figure 1 and R refers to Rhinophrynidae.

Xenopus from Ethiopia also recovered estimates that were in the millions for each species, probably also as a consequence of ancestral population structure (Evans et al. 2011). Another possibility is that gene flow among lineages occurred after speciation via hybridization. The models assumed by BEST and *BEAST do not include gene flow after speciation and this biological phenomenon could lead to inflated estimates of ancestral effective population size by increasing genealogical discordance. Interspecies hybridization during pipoid diversification also seems plausible in light of the frequent allopolyploid evolution in *Xenopus* and *Silurana*.

There are analytical caveats to the multilocus coalescent methods we used. First, these methods generally assume neutral evolution of the data. Here, we included synonymous and nonsynonymous sites in order to maximize the phylogenetic signal of the data and because of the concern that synonymous substitutions would be saturated over the protracted divergence between the ingroup and outgroup (>300 Ma in total; Fig. 6). However, rates of evolution of each codon position strongly suggest nonneutral evolution, minimally of the first and second positions which evolve slower than the third position (Supplementary Fig. 1). It is not yet clear to what degree the inclusion of nonsynonymous sites affected our inference of topology or parameter estimates (including divergence time and effective population size) using these methods and undoubtedly future research will explore this issue. A second important concern relates to the possibility that we included nonorthologous sequences in these alignments (Figs. 3 and 4B). This is difficult to quantify and could account for the inflated estimates of ancestral population size recovered from *BEAST and also for some of the genealogical discordance observed from the analysis of individual loci (Fig. 5). We attempted to cope with this problem using the standardized outgroup distance ratio but it is not clear to what degree, if any, we succeeded. Another concern is that divergence times are partially confounded with ancestral population size due to ancestral polymorphism. Intraspecific sampling would permit the estimation of extant population sizes and potentially improve accuracy of the estimates of ancestral population sizes and divergence times. Simulation studies (J. Heled, unpublished results) suggest that the credible intervals for divergence times and effective population sizes of internal nodes tend to be larger with only one extant sequence per species as compared with analyses with more than one per extant species. Another caveat is that we were unable to achieve convergence with *BEAST analysis using the GTR codon model. This presumably is either because the data were insufficient to inform the posterior distributions of the many parameters in this model, or because we did not run the analysis for long enough or some combination of these possibilities. In a few of the GTR codon runs, we observed large improvements in likelihood that were not achieved in the other runs. We note that while convergence was not achieved for this model, the most strongly supported topology sampled in this high likelihood parameter space was the same as that recovered from the other *BEAST and BEST analyses—that is the ((*Xenopus*, *Silurana*)(*Hymenochirus*, *Pipa*)) topology.

Biogeographical Implications

Dispersal of frog lineages can occur over marine barriers (e.g., Evans et al. 2003; Vences et al. 2003; Heinicke et al. 2007), although this is clearly much less frequent than dispersal over most terrestrial habitats. Here, we consider 2 marine barriers (the separation of South America and Africa ~100 Ma and the separation of North America from West Africa ~190 Ma) to calibrate our divergence estimates. In doing so, we generated hypotheses and associated divergence time predictions that can be independently evaluated using other information.

At least 2 lines of evidence would reject the hypotheses associated with the calibration points in our *BEAST analyses. The first would be evidence of either *Hymenochirus* or *Pipa* on both sides of the Atlantic Ocean, evidence of Rhinophrynidae in Africa, or evidence of Pipidae in North America. To our knowledge, there is no such evidence. The second would be if date estimates

TABLE 2. Pipid fossils can be used to assess credibility of divergence times estimated using geological calibrations of *BEAST analysis 1 (Pipa), *BEAST analysis 2 (Root), and *BEAST analysis 3 (Pipa + Root); for each geological calibration, the credible intervals of estimated divergence times either agree (Y) or do not agree (N) with the estimated sister taxon (Sister) and age (Age) of each fossil taxon by being older and not overlapping or by overlapping, respectively, with the age of the fossils

Fossil	Location	Age	Sister	Citation	Pipa	Root	Pipa + Root
Avitabatrachus uliana	Argentina	Late Albian–Early Cenomanian (112.0–93.5 Ma)	Pipidae, not Rhinophrynidae	Báez et al. (2000); Nevo (1969); Trueb and Báez (2006)	Y	Y	Y
Palaeobatrachus	Europe	Late Cretaceous (99.6–65.6 Ma)	Pipidae, not Rhinophrynidae	Báez et al. (2000); Nevo (1969); Trueb and Báez (2006)	Y	Y	Y
Thoraciliacus	Israel	Early Cretaceous (145.5–99.6 Ma)	Pipidae, not Rhinophrynidae	Báez et al. (2000); Nevo (1969); Trueb and Báez (2006)	N	Y	Y
Cordicephalis	Israel	Early Cretaceous (145.5–99.6 Ma)	Pipidae, not Rhinophrynidae	Báez et al. (2000); Nevo (1969); Trueb and Báez (2006)	N	Y	Y
Shomronella jordanica	Israel	Early Cretaceous (145.5–99.6 Ma)	Pipidae, not Rhinophrynidae	Estes et al. (1978)	N	Y	Y
Rhadinosteus parvus	USA (Utah)	Kimmeridigian (155.7–150.8 Ma)	Rhinophrynidae, not Pipidae	Henrici (1998)	N	Y	Y
Saltenia ibanezi	Argentina	Santonian-Campanian (85.7–70.6 Ma)	Xenopodiane, not Pipinae	Báez and Pugener (2003); Trueb and Báez (1997); Trueb and Báez (2006)	Y	Y	Y
Shelania	Chile + other parts of South America	Palaeogene (65.5–23.0 Ma)	Xenopodiane, not Pipinae	Báez and Pugener (2003); Trueb and Báez (1997); Trueb and Báez (2006)	Y	Y	Y
Llankibatrachus	Chile + other parts of South America	Palaeogene (65.5–23.0 Ma)	Xenopodiane, not Pipinae	Báez and Pugener (2003); Trueb and Báez (1997); Trueb and Báez (2006)	Y	Y	Y
"Xenopus" romeri	Brazil	Palaeocene (65.5–55.8 Ma)	Xenopodiane, not Pipinae	Báez and Pugener (2003); Trueb and Báez (1997); Trueb and Báez (2006)	Y	Y	Y
Xenopus arabiensis	Yemen	Late Oligocene (28.4–23.0 Ma)	Xenopus, not Silurana	Estes (1977); Henrici and Báez (2001)	Y	Y	Y
Eoxenopoides reuningi	South Africa	Maastrichtian/ Selandian (70.6–58.7 Ma)	Pipinae, not Xenopodinae	Báez and Harrison (2005); Báez and Pugener (2003); Trueb and Báez (2006); Trueb et al. (2005)	Y	Y	Y
Vulcanobatrachus mandelai	South Africa	Senonian (89.3–65.5 Ma)	Pipinae, not Xenopodinae	Báez and Harrison (2005); Báez and Pugener (2003); Trueb and Báez (2006); Trueb et al. (2005)	Y	Y	Y
Singidella latecostata	Tanzania	~45 Ma	*Hymenochirus*, not *Pipa*	Báez and Harrison (2005); Báez and Rage (1998); Trueb and Báez (2006)	Y	Y	Y
Pachycentrata (*Pachybatrachus*) *taqueti*	Niger	Coniacian-Santonian (89.3–83.5 Ma)	*Hymenochirus*, not *Pipa*	Báez and Harrison (2005); Báez and Rage (1998); Trueb and Báez (2006)	Y	Y	Y

recovered from these analyses were inconsistent with the fossil or geological record. To explore this further, we compared the fossil record and associated inferences about phylogenetic relationships to our geologically calibrated estimates of divergence times from *BEAST Analyses 1–3 (Table 2). For the most part, the timing and inferred phylogenetic affinities of fossil taxa agreed with the BEST and *BEAST analyses. However, there were some discrepancies between the age and inferred phylogenetic affinities from the fossil record and the 95% credible intervals for the divergence time between Rhinophrynidae and Pipidae that were recovered from *BEAST analysis 1 (Table 2). In particular, the extinct taxa *Thoraciliacus*, *Cordicephalis*, and *Shomronella* from the Early Cretaceous (145.5–99.6 Ma) of Israel, are postulated to be more closely related to Pipidae than to Rhinophrynidae (Nevo 1969; Estes et al. 1978; Báez et al. 2000; Trueb and Báez 2006). These fossils and their inferred relationships suggest that the most recent common ancestor of these fossils and Pipidae diverged from Rhinophrynidae prior to ~145.5 Ma. This time overlaps with the 95% credible interval for the divergence of these clades from *BEAST analysis 1 (115.7–176.4 Ma). Similarly, a fossil of the extinct species *Rhadinosteus parvus* from the Kimmeridigian (155.7–150.8 Ma) is thought to be more closely related

to extant Rhinophrynidae than to extant Pipidae, suggesting that these families diverged before this (Henrici 1998). However, again, the 95% credible interval for the divergence of these clades from *BEAST analysis 1 overlaps with this time.

If migration over marine barriers is difficult for these frogs, the estimated time of divergence of Pipidae from Rhinophrynidae from *BEAST Analysis 1 also is inconsistent with the geological record which indicates that by this time North America had already drifted apart from West Africa forming the North Atlantic Ocean, (Fig. 2; McHone and Butler 1984), which eventually connected with the Tethys Sea to circumscribe the globe. This suggests that the calibrations used in *BEAST Analyses 2 and 3 are most appropriate if the North Atlantic Ocean was a formidable barrier to amphibian dispersal that triggered diversification of pipoids (Duellman and Trueb 1994). While we do not know which of these 2 sets of divergence times are more accurate, the estimated divergence times of Xenopodinae are very similar in *BEAST analyses 2 and 3: ∼65 Ma with a 95% credible intervals of ∼57–76 Ma. These results underscore how ancient various pipid diversification events are, including the age of the subfamily Xenopodinae. Underestimates of divergence, for example by Bisbee et al. (1977), have contributed to nomenclatural confusion associated with the nonubiquitous recognition of "*Silurana*."

Although it does not speak to the validity of the geological calibration points, it is interesting that some fossils from South America are purportedly more closely related to Xenopodinae than to Pipinae, suggesting that both of these lineages were widely dispersed over West Gondwana prior to its breakup (Báez and Pugener 2003; Trueb et al. 2005; Trueb and Báez 2006), even though today Xenopodinae is found only in Africa. An interesting direction for future research would be to add data from divergent taxa within these clades, such as *Pseudhymenochirus merlini* (Cannatella and Trueb 1988b), *Pipa parva* (Cannatella and Trueb 1988a), or *X. borealis* (Evans 2008) in order to provide more detailed information about the timing of diversification within pipids.

Conclusions

We generated a phylogenomic data set with an aim of providing further resolution to ancient relationships among a group of frogs (family Pipidae). In compiling these data, we encountered challenges with data quality in that next generation sequence reads from an old sample of *R. dorsalis* were generally shorter and sparser than those from fresh samples. We encountered challenges with alignment, which drove us to conservatively discard noncoding sequences and randomly discard one *X. laevis* paralog when 2 were identified. In the interest of being confident in our alignments and to avoid violation of model assumptions, we further discarded data from loop regions and one side of stem regions of ribosomal genes from mitochondrial DNA. Despite these conservative measures, the final data set was sufficiently large that it proved difficult to analyze using a relatively complex model, forcing us to resort to a model with less parameters. The ((*Xenopus*, *Silurana*)(*Pipa*, *Hymenochirus*)) topology was recovered using 2 multilocus coalescent methods and multiple models, and this topology was also suggested by analysis of individual loci and a concatenated analysis. Calibration regimes that included a role for the opening of the North Atlantic Ocean ∼190 Ma produced divergent time estimates that were consistent with the fossil record. Perhaps most striking was the high degree of genealogical discordance, which probably stems from a combination of phylogenetic error, inadvertent analysis of nonorthologous (paralogous) data, and large or structured ancestral population sizes. Together, these findings highlight the exciting prospects for the field of phylogenomics and also the daunting analytical challenges that lie ahead.

Supplementary Material

Supplementary material, including data files and/or online-only appendices, can be found in the Dryad data repository (doi: 10.5061/dryad.bt92r9f1).

Funding

This research was supported by a National Science and Engineering Research Council of Canada Discovery Grant and Graduate Fellowship, an Ontario Graduate Fellowship (Internal Prestige Scholarship), an Early Researcher Award from the Ontario Ministry of Economic Development and Innovation, and McMaster University.

Acknowledgements

We thank Jim McGuire for suggesting that we try to extract RNA from a *R. dorsalis* sample at the Museum of Vertebrate Zoology and for providing this tissue loan, Brian Golding for use of computational resources, and Ron DeBry, David Blackburn, Rich Glor, Laura Kubatko, and 3 anonymous reviewers for helpful discussion and comments on an earlier version of this manuscript.

References

Ali J.R., Aitchison J.C. 2008. Gondwana to Asia: plate tectonics, paleogeography and the biological connectivity of the Indian subcontinent from the Middle Jurassic through latest Eocene (166–35 Ma). Earth-Sci. Rev. 88:145–166.

Altschul S.F., Madden T.L., Schaffer A.A., Zhang J., Zhang Z., Miller W., Lipman D.J. 1997. Gapped BLAST and PSI-BLAST: a new generation of protein database search programs. Nucleic Acids Res. 25:3389–3402.

Báez A.M., Harrison T. 2005. A new pipine frog from an Eocene crater lake in North-Central Tanzania. Palaeontology 48:723–737.

Báez A.M., Pugener L.A. 2003. Ontogeny of a new Palaeogene pipid frog from southern South America and xenopodinomorph evolution. Zool. J. Linn. Soc. 139:439–476.

Báez A.M., Rage J. 1998. Pipid frogs from the upper Cretaceous of In Beceten, Niger. Palaeontology 41:669–691.

Báez A.M., Trueb L., Calvo J.O. 2000. The earliest known pipoid frog from South America: a new genus from the middle Cretaceous of Argentina. J. Vert. Paleontol. 20:490–500.
Bewick A.J., Anderson D.W., Evans B.J. 2011. Evolution of the closely related, sex-related genes DM-W and DMRT1 in African clawed frogs (*Xenopus*). Evolution 65:698–712.
Bisbee C.A., Baker M.A., Wilson A.C., Hadji-Azimi I., Fischberg M. 1977. Albumin phylogeny for clawed frogs (*Xenopus*). Science 195:785–787.
Brooks D.R., McLennan D.A. 2002. The nature of diversity. Chicago (IL): Chicago University Press.
Brown W.M., Prager E.M., Wang A., Wilson A.C. 1982. Mitochondrial DNA sequences of primates: tempo and mode of evolution. J. Mol. Evol. 18:225–239.
Cannatella D.C., de Sá R.O. 1993. *Xenopus laevis* as a model organism. Syst. Biol. 42:476–507.
Cannatella D.C., Trueb L. 1988a. Evolution of pipoid frogs: intergeneric relationships of the aquatic frog family Pipidae (Anura). Zool. J. Linn. Soc. 94:1–38.
Cannatella D.C., Trueb L. 1988b. Evolution of pipoid frogs: morphology and phylogenetic relationships of *Pseudhymenochirus*. J. Herpetol. 22:439–456.
Cannone J.J., Subramanian S., Schnare M.N., Collett J.R., D'Souza L.M., Du Y., Feng B., Lin N., Madabusi L.V., Muller K.M., Pande N., Shang Z., Yu N., Gutell R.R. 2002. The comparative RNA web (CRW) site: an online database of comparative sequence and structure information for ribosomal, intron, and other RNAs. BioMed Central Bioinformatics 3:2.
Chain F.J.J., Dushoff J., Evans B.J. 2011. The odds of duplicate gene persistence after polyploidization. BMC Genomics 12:599.
Chain F.J.J., Evans B.J. 2006. Multiple mechanisms promote the retained expression of gene duplicates in the tetraploid frog Xenopus laevis. PLoS Genet. 2:e56.
Chain F.J.J., Ilieva D., Evans B.J. 2008. Duplicate gene evolution and expression in the wake of vertebrate allopolyploidization. BMC Evol. Biol. 8:43.
Degnan J.H., Rosenberg N.A. 2006. Discordance of species trees with their most likely gene trees. PLoS Genet. 2:e68.
Degnan J.H., Rosenberg N.A. 2009. Gene tree discordance, phylogenetic inference and the multispecies coalescent. Trends Ecol. Evol. 24:332–340.
Degnan J.H., Salter L.A. 2005. Gene tree distributions under the coalescent process. Evolution 59:24–37.
Drummond A.J., Rambaut A. 2007. BEAST: Bayesian evolutionary analysis by sampling trees. BMC Evol. Biol. 7:214.
Duellman W.E., Trueb L. 1994. Biology of amphibians. Baltimore (MD): The Johns Hopkins University Press.
Edgar R.C. 2004. MUSCLE: a multiple sequence alignment method with reduced time and space complexity. BMC Bioinformatics 5:115.
Estes R. 1977. Relationships of the South African fossil frog *Eoxenopoides reuningi* (Anura, Pipidae). Annals of the South African Museum 73:49–80.
Estes R., Spinar Z.V., Nevo E. 1978. Early Cretaceous pipid tadpoles from Israel (Amphibia: Anura). Herpetologica 34:374–393.
Evans B.J. 2007. Ancestry influences the fate of duplicated genes millions of years after duplication in allopolyploid clawed frogs (*Xenopus*). Genetics 176:1119–1130.
Evans B.J. 2008. Genome evolution and speciation genetics of allopolyploid clawed frogs (*Xenopus* and *Silurana*). Front. Biosci. 13: 4687–4706.
Evans B.J., Bliss S.M., Mendel S.A., Tinsley R.C. 2011. The Rift Valley is a major barrier to dispersal of African clawed frogs (Xenopus) in Ethiopia. Mol. Ecol. 20:4216–4230.
Evans B.J., Brown R.M., McGuire J.A., Supriatna J., Andayani N., Diesmos A., Iskandar D.T., Melnick D.J., Cannatella D.C. 2003. Phylogenetics of Fanged Frogs (Anura; Ranidae; *Limnonectes*): testing biogeographical hypotheses at the Asian-Australian faunal zone interface. Syst. Biol. 52:794–819.
Evans B.J., Kelley D.B., Melnick D.J., Cannatella D.C. 2005. Evolution of RAG-1 in polyploid clawed frogs. Mol Biol. Evol. 22:1193–1207.
Evans B.J., Kelley D.B., Tinsley R.C., Melnick D.J., Cannatella D.C. 2004. A mitochondrial DNA phylogeny of clawed frogs: phylogeography on sub-Saharan Africa and implications for polyploid evolution. Mol. Phylogenet. Evol. 33:197–213.
Ford L.S., Cannatella D.C. 1993. The major clades of frogs. Herpetological Monographs 7:94–117.
Frost D.R. 2011. Amphibian species of the world: an online reference. Version 5.5. New York: American Museum of Natural History.
Frost D.R., Grant T., Faivovich J., Bain R.H., Haas A., Haddad C.F.B., De Sá R., Channing A., Wilkinson M., Donnellan S.C., Raxworthy C.J., Campbell J.A., Blotto B.L., Moler P., Drewes R.C., Nussbaum R.A., Lynch J.D., Green D.M., Wheeler W.C. 2006. The amphibian tree of life. American Museum of Natural History 297:1–370.
Gheerbrant E., Rage J. 2006. Paleobiogeography of Africa: how distinct from Gondwana and Laurasia? Palaeogeogr. Palaeoclimatol. Palaeoecol. 241:224–246.
Graf J.D. 1996. Molecular approaches to the phylogeny of *Xenopus*. In: Tinsley R.C., Kobel H.R., editors. The biology of *Xenopus*. Oxford: Clarendon Press. p. 379–389.
Heinicke M.P., Duellman W.E., Hedges S.B. 2007. Caribbean and Central American frog faunas originated by ancient oceanic dispersal. Proc. Natl Acad. Sci. U. S. A. 104:10092–10097.
Heled J., Drummond A.J. 2010. Bayesian inference of species trees from multilocus data. Mol Biol. Evol. 27:570–580.
Heled J., Drummond A.J. 2011. Calibrated tree priors for relaxed phylogenetics and divergence time estimation. Syst. Biol. doi: 10.1093/sysbio/syr087.
Hellsten U., Khokha M.K., Grammer T.C., Harland R.M., Richardson P., Rokhsar D.S. 2007. Accelerated gene evolution and subfunctionalization in the pseudotetraploid frog *Xenopus laevis*. BMC Evol. Biol. 5:31.
Henrici A.C. 1998. A new pipoid anuran from the Late Jurassic Morrison Formation at Dinosaur National Monument, Utah. J. Vert. Paleont. 18:321–332.
Henrici A.C., Báez A.M. 2001. First occurrence of *Xenopus* (Anura: Pipidae) on the Arabian Peninsula: a new species from the Late Oligocene of the Republic of Yemen. J. Paleont. 75:870–882.
Hillis D.M., Huelsenbeck J.P., Cunningham C.W. 1994. Application and accuracy of molecular phylogenies. Science 264:671–677.
Huang H., Knowles L.L. 2009. What is the danger of the anomaly zone for empirical phylogenetics? Syst. Biol. 58:527–536.
Huelsenbeck J.P., Ronquist F. 2001. MrBayes: Bayesian inference of phylogenetic trees. Bioinformatics 17:754–755.
Ioerger T.R., Clark A.G., Kao T.-H. 1990. Polymorphism at the self-incompatibility locus in Solanaceae predates speciation. Proc. Natl Acad. Sci. U. S. A. 87:9732–9735.
Irisarri I., Vences M., San Mauro D., Glaw F., Zardoya R. 2011. Reversal to air-driven sound production revealed by a molecular phylogeny of tongueless frogs, family Pipidae. BMC Evol. Biol. 11:114.
Kass R.E., Raftery A.E. 1995. Bayes factors. J. Amer. Statist. Assoc. 90:773–795.
Kluge A.G., Farris J.S. 1969. Quantitative phyletics and evolution of the anurans. Syst. Zool. 18:1–32.
Kobel H., Barandun B., Thiebaud C.H. 1998. Mitochondrial rDNA phylogeny in *Xenopus*. Herpetol. J. 8:13–17.
Korte C., Hesselbo S.P., Jenkyns H.C., Rickaby R.E.M., Spötl C. 2009. Palaeoenvironmental significance of carbon- and oxygen-isotope stratigraphy of marine Triassic Jurassic boundary sections in SW Britain. J Geol. Soc. 166:431–445.
Kubatko L.S., Degnan J.H. 2007. Inconsistency of phylogenetic estimates from concatenated data under coalescence. Syst. Biol. 56: 17–24.
Liu L., Pearl D.K. 2007. Species trees from gene trees: reconstructing Bayesian posterior distributions of a species phylogeny using estimated gene tree distributions. Syst Biol. 56:504–514.
Lynch J.D. 1973. The transition from archaic to advanced frogs. In: Vial J.L., editor. Evolutionary biology of anurans: contemporary research on major problems. Columbia: University of Missouri Press. p. 133–182.
Maddison D.R., Maddison W.P. 2000. MacClade. 4.0 ed. Sunderland (MA): Sinauer Associates.
Maddison W.P. 1997. Gene trees in species trees. Syst. Biol. 46:523–536.
Maisey J.G. 2000. Continental break up and the distribution of fishes of Western Gondwana during the Early Cretaceous. Cretaceous Research 21:281–314.

McHone J.G. 2000. Non-plume magmatism and rifting during the opening of the central Atlantic Ocean. Tectonophysics 316:287–296.
McHone J.G., Butler J.R. 1984. Mesozoic igneous provinces of New England and the opening of the North Atlantic Ocean. Geol. Soc. Am. Bull. 95:757–765.
McLoughlin S. 2001. The breakup history of Gondwana and its impact on pre-Cenozoic floristic provincialism. Aust. J. Bot. 49:271–200.
Morin R.D., Chang E., Petrescu A., Liao N., Griffith M., Kirkpatrick R., Butterfield Y.S., Young A.C., Stott J., Barber S., Babakaiff R., Dickson M.C., Matsuo C., Wong D., Yang G.S., Smailus D.E., Wetherby K.D., Kwong P.N., Grimwood J., Brinkley C.P., Brown-Jogn M., Reddix-Dugue N.D., Mayo M., Schnmutz J., Beland J., Park M., Gibson S., Olson T., Bouffard G.G., Tsai M., Featherstone R., Shand S., Siddiqui A.S., Jang W., Lee E., Klein S.L., Blakesley R.W., Zeeberg B.R., Narasimban S., Weinstein J.N., Pannacchio S.P., Myers R.M., Green E.D., Wagner L., Gerhard D.S., Marra M.A., Jones S.J.M., Holt R.A. 2006. Sequencing and analysis of 10,967 full-length cDNA clones from *Xenopus laevis* and *Xenopus tropicalis* revealspost-tetraploidization transcriptome remodeling. Genome Res. 16: 796–803.
Nei M., Takahata N. 1993. Effective population size, genetic diversity and coalescence time in subdivided populations. J. Mol. Evol. 37:240–244.
Nevo E. 1969. Pipid frogs from the Early Cretaceous of Israel and pipid evolution. Bulletin of the Museum of Comparative Zoology 136: 255–218.
Nylander J.A.A. 2004. MrModeltest v2. Evolutionary Biology Centre, Uppsala University, Uppsala, Sweden.
Nylander J.A.A., Ronquist F., Huelsenbeck J.P., Nieves-Aldrey J.L. 2004. Bayesian phylogenetic analysis of combined data. Syst. Biol. 53:47–67.
Pitman W.C. III, Cande S., LaBrecque J., Pindell J. 1993. Fragmentation of Gondwana: the separation of Africa from South America. In: Goldblatt P., editor. Biological relationships between Africa and South America. New Haven (CT): Yale University Press. p. 15–34.
Pyron R.A., Wiens J.J. 2011. A large-scale phylogeny of Amphibia including over 2800 species, and a revised classification of extant frogs, salamanders, and caecilians. Mol. Phylogenet. Evol. 61(2):543–583.
Roelants K., Bossuyt F. 2005. Archaeobatrachian paraphyly and Pangean diversification of crown-group frogs. Syst. Biol. 54: 111–126.
Roelants K., Gower D.J., Wilkinson M., Loader S.P., Biju S.D., Guillaume K., Moriau L., Bossuyt F. 2007. Global patterns of diversification in the history of modern amphibians. Proc. Natl Acad. Sci. U. S. A. 104:887–892.
Rosenberg N.A. 2002. The probability of topological concordance of gene trees and species trees. Theor. Popul. Biol. 61: 225–247.
Sémon M., Wolfe K.H. 2008. Preferential subfunctionalization of slow-evolving genes after allopolyploidization in *Xenopus laevis*. Proc. Natl Acad. Sci. 105:8333–8338.
Sereno P.C., Wilson J.A., Conrad J.L. 2004. New dinosaurs link southern landmasses in the Mid-Cretaceous. Proc. R Soc. Lond. Series B 271:1325–1330.
Smith A.G., Smith D.G., Funnell B.M. 1994. Atlas of Mesozoic and Cenozoic coastlines. Cambridge: Cambridge University Press.
Sukumaran J., Linkem C.W. 2009. Choice of topology estimators in Bayesian phylogenetic analysis. Mol. Biol. Evol. 26:1–3.
Swofford D.L. 2002. Phylogenetic analysis using parsimony (* and other methods). Version 4. Sunderland (MA): Sinauer Associates.
Trueb L., Báez A.M. 1997. Redescription of the Paleogene *Shelania pascuali* from Patagonia and its bearing on the relationships of fossil and Recent pipoid frogs. Scientific Papers, Natural History Museum, University of Kansas. 4:1–41.
Trueb L., Báez A.M. 2006. Revision of the Early Cretaceous *Cordicephalus* from Israel and an assessment of its relationships among pipoid frogs. J. Vert. Paleont. 26:44–59.
Trueb L., Cannatella D.C. 1986. Systematics, morphology, and phylogeny of genus *Pipa* (Anura: Pipidae). Herpetologica 42:412–449.
Trueb L., Ross C.F., Smith R. 2005. A new pipoid anuran from the Late Cretaceous of South Africa. J. Vert. Paleont. 25:533–547.
Vences M., Vieites D.R., Glaw F., Brinkmann H., Kosuch J., Veith M., Meyer A. 2003. Multiple overseas dispersal in amphibians. Proc. Royal Soc. Lond. B 270:2435–2442.
Wiens J.J. 2011. Re-evolution of lost mandibular teeth in frogs after more than 200 million years, and re-evaluating Dollo's Law. Evolution 65:1283–1296.
Withjack M.O., Schlische R.W., Olsen P.E. 1998. Diachronous rifting, drifting, and inversion on the passive margin of Central Eastern North America: an analog for other passive margins. AAPG Bulletin 82:817–835.
Wong K.M., Suchard M.A., Huelsenbeck J.P. 2008. Alignment uncertainty and genomic analysis. Science 319:473–476.
Wright S. 1943. Isolation by distance. Genetics 28:114–138.